Experimental study on cyclic behavior of reinforced concrete parallel redundancy walls

Yiqiu Lu[a] and Liang Huang[*]

Department of Civil Engineering, Hunan University, Changsha, 410082, China

Abstract. Reinforced concrete (RC) shear walls are one of the most commonly used lateral-load resisting systems in high-rise buildings. RC Parallel redundancy walls studied herein consist of two parts nested to each other. These two parts have different mechanical behaviors and energy dissipation mechanisms. In this paper, experimental studies of four 1/2-scale specimens representing this concept, which are subjected to in-plane cyclic loading, are presented and test results are discussed. Two specimens consist of a wall frame with barbell-shaped walls embedded in it, and the other two consist of a wall frame and braced walls nested each other. The research mainly focuses on the failure mechanism, strength, hysteresis loop, energy dissipation capacity and stiffness of these walls. Results show that the RC parallel redundancy wall is an efficient lateral load resisting component that acts as a "dual" system with good ductility and energy dissipation capacity. One main part absorbs a greater degree of the energy exerted by an earthquake and fails first, whereas the other part can still behave as an independent role in bearing loads after earthquakes.

Keywords: experimentation; redundancy; shear walls; earthquakes; failure mechanism; dual system

1. Introduction

The theory of redundancy has gained wide attention among structural engineers and researchers after the poor performance of some building structures caused by poor system behavior under natural earthquakes or other hazards (Kanno and Ben-Haim 2011, Liao *et al*. 2007, Wen and Song 2003). This has already been recognized by current codes, which stipulate that structures should have redundancy and multi-load transfer path when the structures are required to resist large lateral load due to ground motions caused by earthquakes. For example, a redundancy factor, introduced in NEHRP (1997), UBC-97 (ICBO 1997) is used as a multiplier of the lateral design earthquake load and a more mechanism-based factor is recommended in NEHRP (2003) and adopted in ASCE-7 (2005). Structures are more reliable in accordance with these new design concepts. However, how to design redundant structures is still a significant research topic.

Shear walls are widely recognized for providing adequate lateral load resistance and drift control for high-rise buildings in seismic regions. Actually, the concept of redundancy has already been used in composite and hybrid wall systems which consists a frame as a boundary and a wall

---

[*]Corresponding author, Associate Professor, E-mail: lianghuanghnu@gmail.com
[a]Master, E-mail: lyqhnu@gmail.com

<div align="center">(a) traditional system   (b) parallel redundancy system</div>

<div align="center">Fig. 1 Traditional and parallel redundancy systems</div>

inside. The boundary can restrain the inside wall effectively in the earthquakes. They can still bear loads after the infill wall is damaged, acting as a dual system. Numerous tests of composite walls have verified this behavior. (Zhao and Astaneh-Asl 2004, Tong *et al*. 2005, Sun *et al*. 2011, Berman and Bruneau 2005, Qu *et al*. 2008, Clayton *et al*. 2012)

For reinforced concrete (RC) structural walls, the concept of redundancy has not been recognized widely. Although there has been a significant amount of research on innovative shear walls to improve its seismic behavior, such as RC coupled shear wall with concealed bracings proposed by Dong (2002), RC walls with welded wire mesh tested by Riva and Franchi (2001), RC walls with diagonal web reinforcement proposed by Sittipuntet *et al*. (2001), slit shear walls by Jiang *et al*. (2003), RC high-rise shear wall with steel frame and concealed truss conducted by Cao *et al*. (2009), a slit shear wall with energy-dissipation devices by Kwan *et al*. (1993), dual function slitted shear wall by Ye and Kang (2000), partial RC shear walls with vulnerable frames by Kaltakci and Yavuz (2012) and etc., the main purpose of designing these walls above is to possess high ductility and energy dissipation capacity, the concept of redundancy has not been introduced in these walls. Once the wall is damaged, there is no residual load path that can transfer load. Due to the disadvantage mentioned above, the progressive collapse of the overall structure is likely to occur during earthquakes. Moreover, the post-earthquake rehabilitation work that focuses on the whole wall also results in repair difficulty and high cost.

In this study, redundancy is introduced to the RC walls by putting forward RC parallel redundancy shear walls. The design concept of this new wall involves two independent walls having different energy dissipation mechanisms. These two parts are nested to each other in order to increase the redundancy of the overall wall. The difference between parallel redundancy wall and RC traditional wall mentioned above can be expressed in Fig. 1 (Cennamo 2012).

Fig. 1(a) presents traditional walls and Fig. 1(b) represents parallel redundancy walls. Compared to traditional walls, parallel redundancy walls may collapse only if all its parts have failed as it is characterized by structural redundancy. But for traditional wall, once the wall is damaged, there is no residual load path that can transfer load, so the progressive collapse of the overall structure is likely to occur during earthquakes. The probability of collapse for a traditional wall and a parallel redundancy wall is remarkably different. Further, it is different with frame-wall structure. The frame-wall structures are dual structures, however, parallel walls studied herein are dual structural components. There are alternative load paths in one structural element.

The parallel redundancy walls designed in this paper consist of two parts. Each part is an independent part that can withstand vertical and lateral loads alone, and can play its own mechanical behavior. Therefore, these two parts will not fail simultaneously. During earthquakes, the weaker part of the parallel redundancy wall will yield and fail first, which dissipates most of the energy. Meanwhile, the other part of the wall can still carry loads as an independent role after the earthquake. Moreover, because of the redundancy in the overall wall, the load path can be alternated after the damage of some elements, which can avoid progressive collapse. These walls

are of great cost efficiency compared to steel plate shear walls and composite walls and also, it is a dual system with redundancy compared with traditional RC walls.

The results of an experimental research on four RC walls representing this concept, which are subjected to cyclic loading, are presented herein. The main objective is to establish the cyclic behavior regarding failure mechanism, strength, hysteresis loop, energy dissipation capacity and stiffness of the walls.

2. Specimen design

Four parallel redundancy specimen walls were designed. All of the four walls had two parts nested to each other. Part I is a wall frame and part II is a RC wall embedded in the wall frame (Fig. 2). The specimens were 1/2-scale two stories and were divided into two categories (Fig. 2).

For FB-1 and FB-2, the embedded walls were designed to yield and fail first and for FS-1 and FS-2, the wall frame was designed to fail first. Therefore, for FB-1 and FB-2, the section of the embedded walls were weakened to be barbell-shaped, so the barbell-shaped walls were expected to yield and fail first. Because of the good excellent energy dissipation capacity of the barbell-shaped walls, the barbell-shaped walls would dissipate a considerable part of earthquake energy and the wall frame was expected to be capable of resisting additional loads after earthquakes. Contrarily, for FS-1 and FS-2, the embed walls were strengthened by concealed bracings so that the wall frame was expected to dissipate energy and fail first. There was a gap of 10 mm between the wall frame and the embedded walls. Specimens FB-1 and FS-1 were one-bay structures with aspect
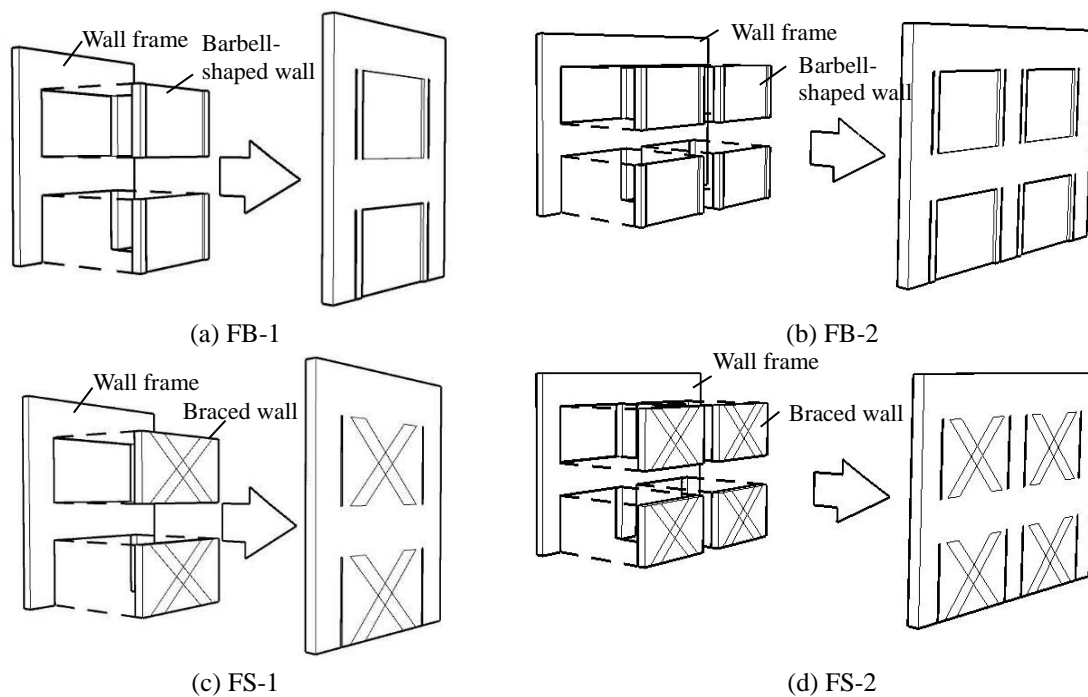

(a) FB-1

(b) FB-2

(c) FS-1

(d) FS-2

Fig. 2 Parallel redundancy walls
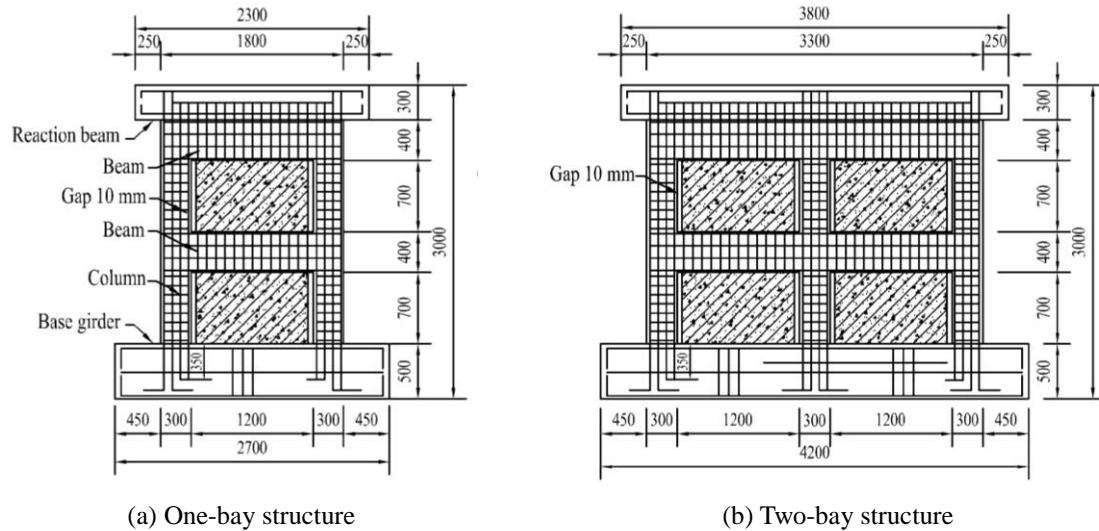
(a) One-bay structure   (b) Two-bay structure

Fig. 3 Geometry of specimens (all dimensions in mm)

Table 1 Material properties of the specimens

Specimen	f_{cu}, MPa	f_{yv1}, MPa	f_{ys1}, MPa	f_{yv2}, MPa	f_{ys2}, MPa
FB-1	46.2	513	638	445	511
FB-2	50.1	513	638	445	511
FS-1	47.1	513	638	445	511
FS-2	44.0	513	638	445	511

f_{cu}=compressive cube (150×150×150 mm) strength of concrete; f_{yv1}=yield strength of Φ6; f_{ys1}= ultimate strength of Φ6; f_{yv2}=yield strength of Φ8; f_{ys2}= ultimate strength of Φ8

ratio 1.3, whereas specimens FB-2 and FS-2 were two-bay structures with aspect ratio 0.71. The overall dimensions of the specimens are shown in Fig. 3. The longitudinal and transverse reinforcement of the beams and columns were all the same in wall frame the four specimens.

Vertical reinforcement was anchored in a 500 mm thick base girder fixed by concrete blocks in both sides. A reaction beam with a width and depth of 200 and 300 mm, respectively, was cast on the top of the wall panel, and a hydraulic actuator was attached to the specimen at the mid-depth of the top beam. Crossed-inclined bars were provided at the connection of the wall frame and the base girder to prevent sliding failure. The material properties of the reinforcement and concrete are summarized in Table 1. Steel reinforcement was detailed in accordance with the current practice in China (GB 50010-2010 and GB5001-2010). The design details of the specimens are shown in Fig. 4. The construction processes are as follows: 1) assemble bar cage for foundation block, including longitudinal reinforcement originating in the foundation; 2) cast concrete for foundation; 3) assemble reinforcement for wall (frame and embedded wall) and top beam; 4) cast wall concrete.

3. Test setup

The test setup is shown in Fig. 5. The testing equipment is capable of applying a maximum

(a) columns   (b) beams   (c) reaction beam   (d) base girder

(e) barbell-shaped walls   (f) barbell-shaped walls

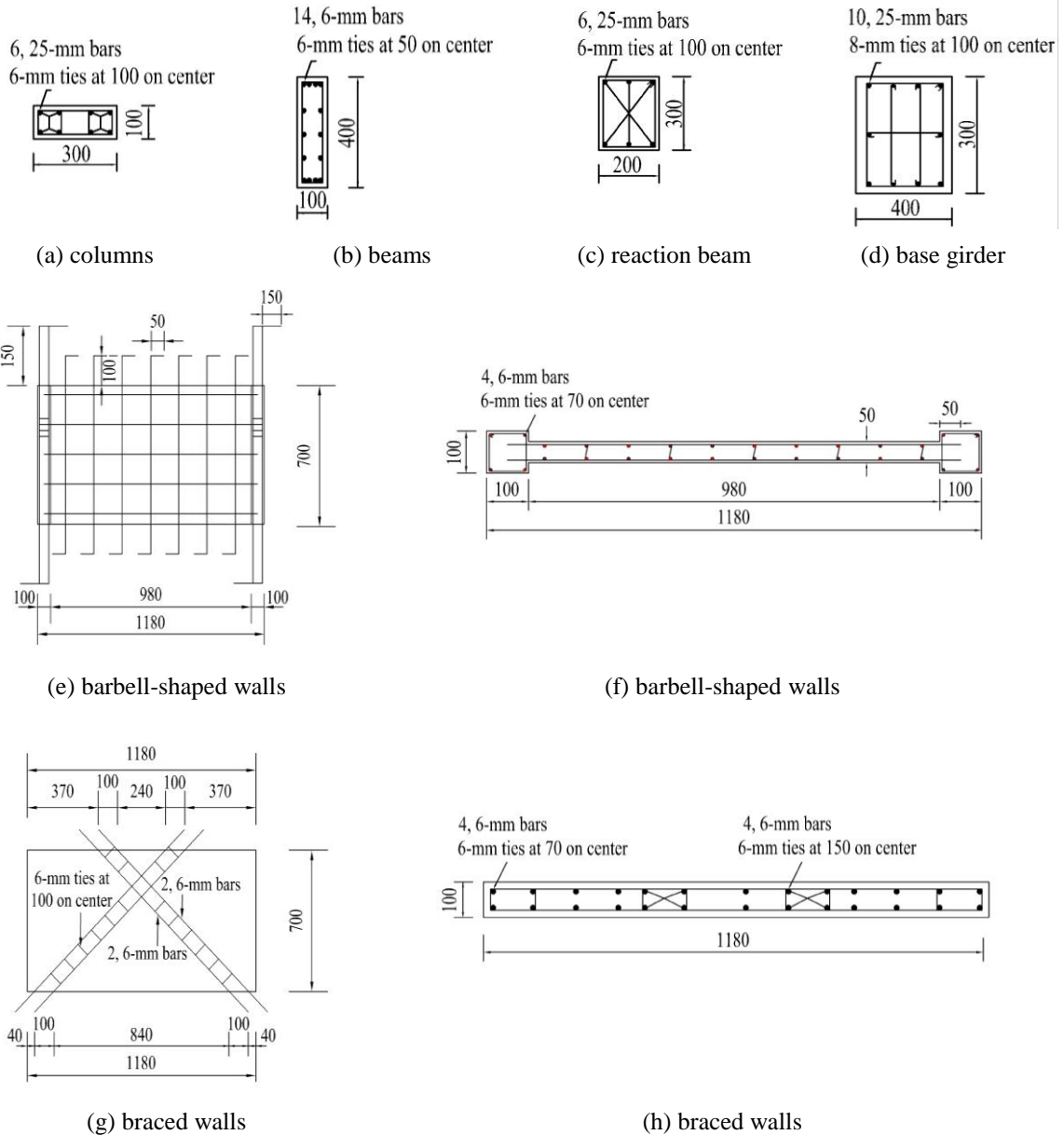(g) braced walls   (h) braced walls

Fig. 4 Specimen details: cross sections and reinforcement (all dimensions in mm)

horizontal force of 1500 kN, with a maximum horizontal displacement of 200 mm, and a vertical force of 600 kN applied by means of a hydraulic jack. The reaction beam and base girder were also designed to simulate the boundary conditions of a shear wall panel in a generic building under seismic effects. To simulate the bracing effects provided by the floors, bracings were applied at the middle beam to prevent out-of-plane movements. Jacks that provided vertical force were placed on the top beam to simulate gravity loading.
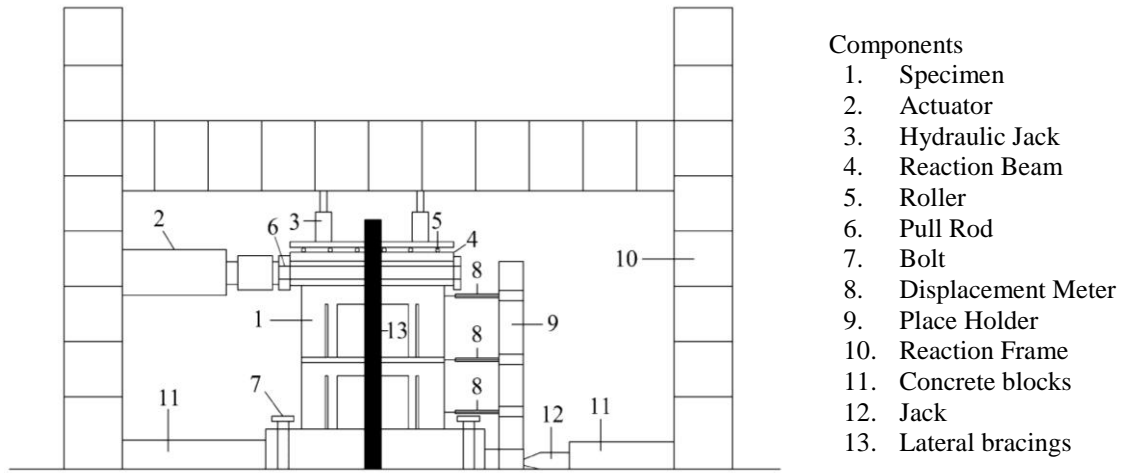
Components
1. Specimen
2. Actuator
3. Hydraulic Jack
4. Reaction Beam
5. Roller
6. Pull Rod
7. Bolt
8. Displacement Meter
9. Place Holder
10. Reaction Frame
11. Concrete blocks
12. Jack
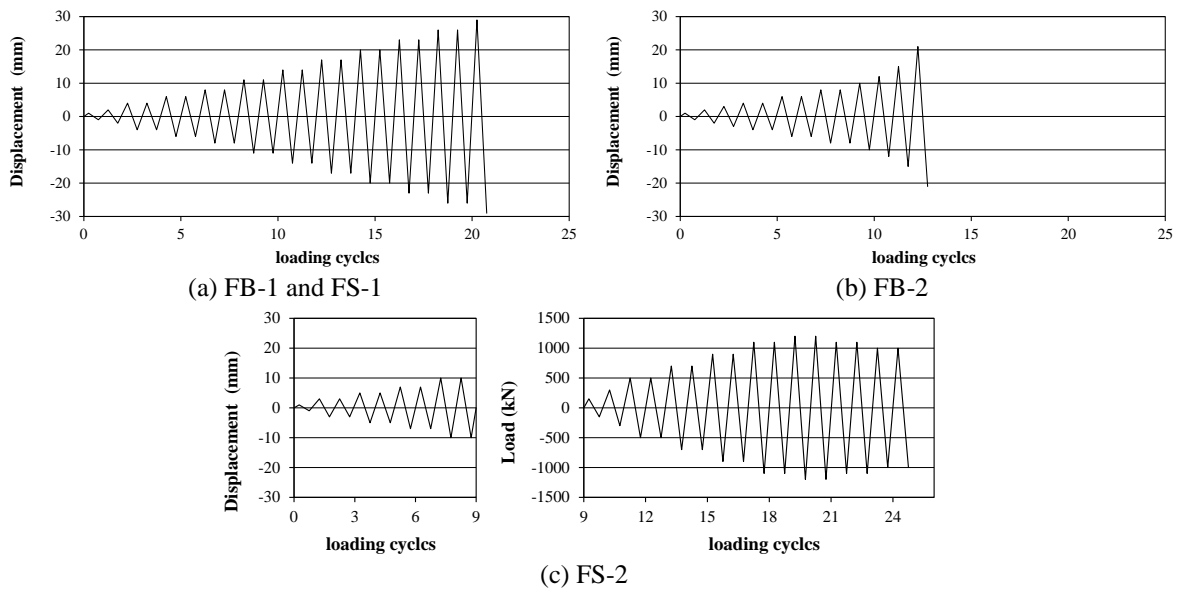13. Lateral bracings

Fig. 5 Test setup

(a) FB-1 and FS-1

(b) FB-2

(c) FS-2

Fig. 6 Loading history for the experimental program

4. Loading history

Cyclic displacements were applied according to the loading history, which began with very small values and gradually increased until the failure of the specimen. Each specimen load cycle consisted of a half cycle in the positive direction and a half cycle in the negative direction. The displacement increment adopted in the loading history was divided into three categories. An increment of 1 mm was adopted to push the specimens to the cracking load in both directions; an increment of 2 mm was used during subsequent cycles to push the specimens to the yield point, such that the top deflection reaches integer multiples of the yield displacement in both directions;

and after the yield point, an increment of 3 mm was adopted to continue the test until the specimen experienced a significant loss of capacity. After the cracking load, each cycle was repeated two times until the specimen was destroyed or the lateral load decreased to 80% of the ultimate load level of the specimen (Park 1989). The axial load adopted for FB-1, FS-1, FB-2, and FS-2 were 100, 100, 600, and 600 kN, respectively. The loading history of specimen FS-2, however, was different from those of the other three specimens. During the test, the bolt connecting the hydraulic servo actuator and the reaction steel frame snapped, hence the test had to be stopped. Due to the concern for the security of the personnel, the axial load was reduced from 600 to 100 kN. In the following text, FS-2' represents FS-2 with axial load of 600 kN and FS-2'' represents FS-2 with axial load of 100 kN. In addition, because there had already been plastic deformation in the wall, load control was used in further tests. Fig. 6 shows the loading history of the four specimens.

5. Instrumentation

Instrumentation was selected to monitor applied loads, deformations, and strains in the reinforcing steel bars. Displacement meters were placed along the height of the specimens to monitor the lateral displacement, as shown in Fig. 5. One was installed at the top of the specimen to monitor top displacement. The second one was installed at a distance of 200 mm from the wall base to measure the sliding of the base. A third one was installed at the middle of the wall to measure the middle displacement.

To measure strains at critical locations on the specimens, strain gauges were mounted on the specimens. Critical locations included the bottom point of vertical steel bars in the columns and the end point of horizontal steel bars in the beams.

## 6. Crack patterns of parallel redundancy walls

The four specimens showed very good cooperative work performance during the test. The crack patterns and failure modes of the four specimens are shown in Figs. 7, 8, 9 and 10. There were some common features among these four specimens.

First, the failure of one part led to the overall damage while the other wall could still bear capacity. For walls FB-1 and FB-2, the wall frame was still in good condition after the failure of the barbell-shaped wall. When the wall failed, the bottom concrete of the barbell-shaped wall was completely damaged. However, the concrete at the bottom of the column was slightly crushed, as can be seen in Figs. 7 and 8, hence it still could bear additional loads after the failure of the barbell-shaped wall. As for walls FS-1 and FS-2, the failure of the wall frame caused the damage of the overall wall, and the braced walls could still bear capacity, as can be seen in Figs. 9 and 10. Thus, hierarchy existed in the failure process of the parallel redundancy walls. If one desires to obtain different seismic behaviors, the embedded wall can be designed to different forms. This behavior is different from that of traditional walls with no separation of primary and secondary parts.

Second, in all specimens, as Figs. 7, 8, 9 and 10 show, the side columns developed horizontal cracks, and the embedded walls and the middle columns developed diagonal shear cracks, indicating the two parts had different dissipation mechanism. Flexural behavior occurred in the side columns while shear behavior occurred in the embedded walls. Such behavior also indicated
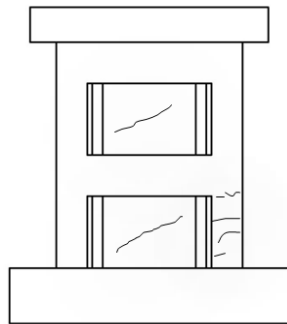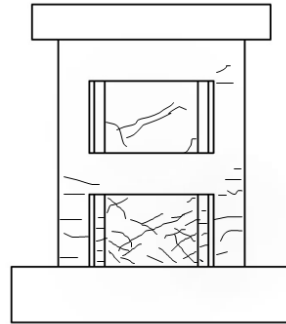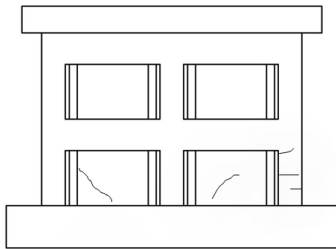
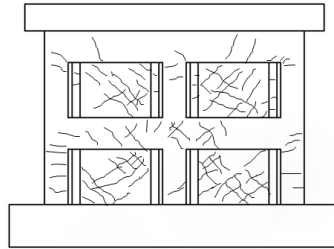| (a) the stage of cracking | (b) the stage of yielding | (c) the stage of failure |

Fig. 7 Crack pattern of FB-1
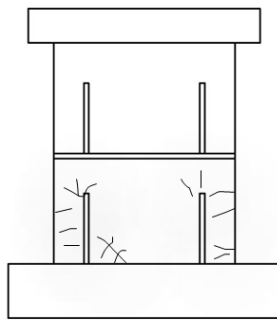

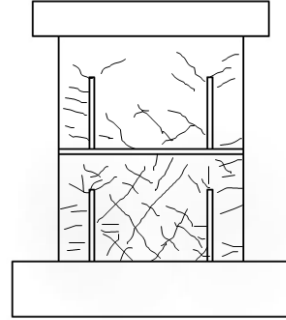| (a) the stage of cracking | (b) the stage of yielding | (c) the stage of failure |

Fig. 8 Crack pattern of FB-2

| (a) the stage of cracking | (b) the stage of yielding | (c) the stage of failure |

Fig. 9 Crack pattern of FS-1

that there is a hierarchy in the process of crack development of parallel redundancy walls under the lateral load. The side columns were separated with the embedded walls and these two parts can behave their different role under lateral loads. The side walls were strong enough that they would not damage seriously under large moments and would not be a vulnerable part in the earthquakes. Even if the side walls failed first, it would not influence the whole wall. However, generally, this crack pattern cannot be found in the ordinary walls when the aspect ratio is similar with the tested walls in this article.

(a) the stage of cracking　　　　　(b) the stage of yielding　　　　　(c) the stage of failure
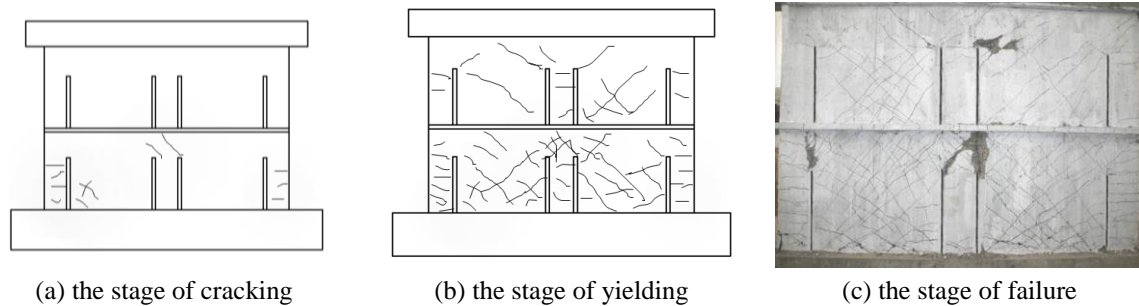
Fig. 10 Crack pattern of FS-2

Third, many cracks also appeared on the second stories of all four walls, which dissipated the cyclic energy. This indicated that the energy dissipation capacity of the second story of the parallel redundancy walls could be effectively utilized.

Specimens FB-1 and FB-2 behaved in a similar manner in the failure process, but differences were still observed during the test. First, for FB-1, the reason for failure of the specimen was the spallation of the concrete at the bottom of the barbell-shaped walls. For FB2, the large shear crack caused the failure of the barbell-shaped walls. This led to a great drop in the horizontal load-carrying capacity of the specimen. Walls FB-1 and FB-2 were basically governed by bending failure and shear failure, respectively, because the aspect ratios of two specimens were 1.3 and 0.71. For the wall beams, more shear cracks were notably observed in FB-2. During the failure process of FB-1, the main damage focused on the concrete at the bottom of the barbell-shaped walls, hence no great damage could be found in the other locations of the wall. However, for FB-2, the wall beams could also behave as a significant role in resisting shear load because the wall beams were surrounded by the four barbell-shaped walls. Thus, there were many shear cracks observed.

The failure of the wall frame caused the overall failure of the wall for both FS-1 and FS-2. The difference was the damage location, where it was the wall columns for FS-1 and the wall beams for FS-2. For FS-2, the greater stiffness and higher lateral capacity enabled the braced walls to provide more lateral shear capacity. Therefore, the wall beams and the braced wall collaboratively resisted shear loads. Finally, the overall wall failed by the damage of the wall beams due to its low capacity compared with the braced wall. However, for FS-1, braced walls resisted less shear loading and the bending load for wall columns was greater than the shear load for wall beams. Hence, the wall columns were damaged and the wall beams remained in good condition.

The major difference between the cyclic behavior of FS-1, FS-2 and FB-1, FB-2 came from the embedded walls. The braced walls were strengthened by the cross bracings while the dimensions of the barbell-shaped walls were weakened. Therefore, at the stage of failure, FB-1 and FB-2 failed by the damage of the barbell-shaped walls, whereas FS-1 and FS-2 failed by the damage of the wall frame.

7. Hysteretic behavior

Fig. 11 shows the hysteresis loops of the four specimens. Two hysteresis loops could be obtained for FS-2 because it was loaded twice with different axial loads. All walls experienced

(a) FB-1

(b) FB-2

(c) FS-1

(d) FS-2 before a drop of axial load
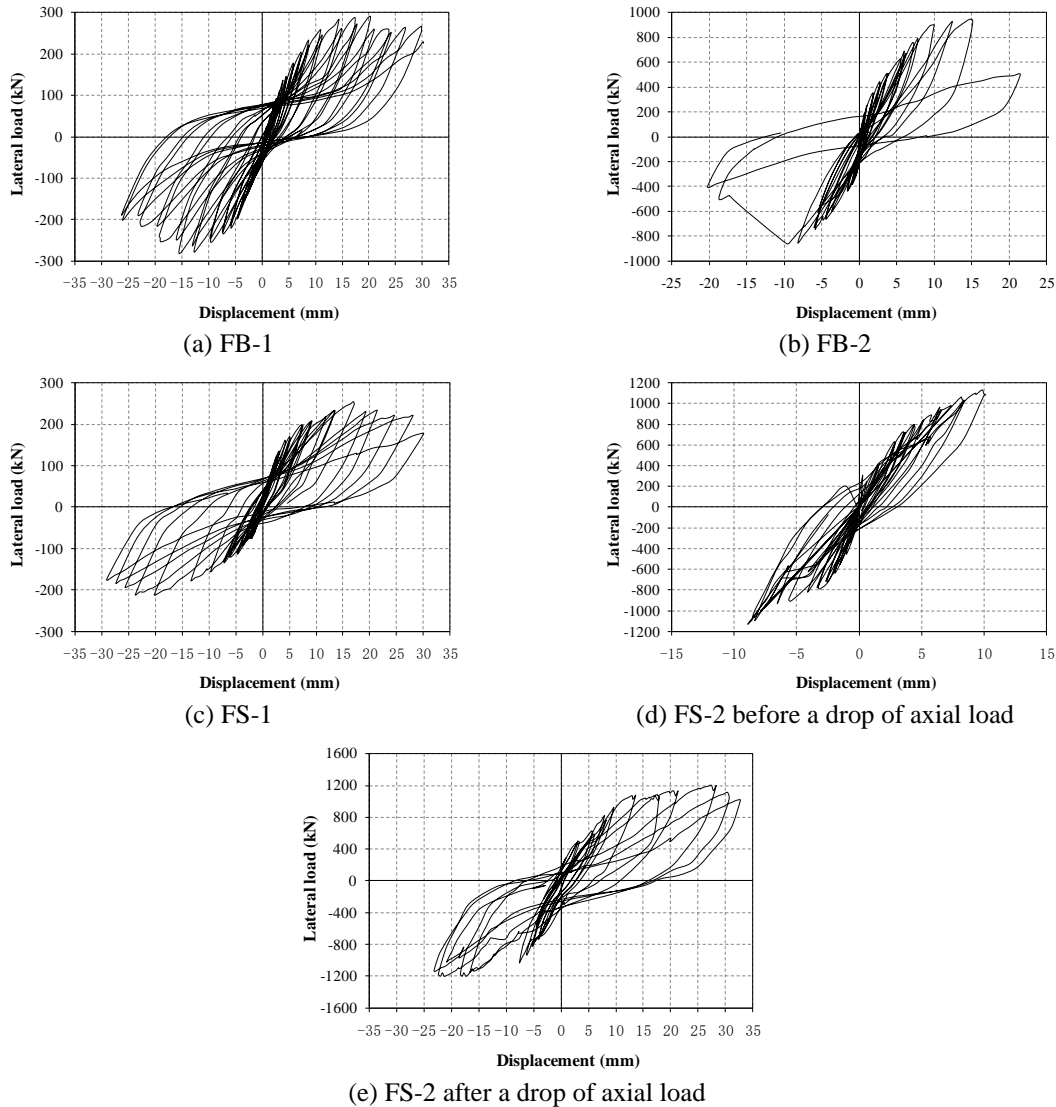
(e) FS-2 after a drop of axial load

Fig. 11 Hysteresis loops of the specimens

stages of cracking, yielding, and failing. Before cracks appeared, the wall was basically elastic and the loading curve overlapped with the unloading curve. After that, the loops formed a spindle shape and its enclosed area was small, which indicated that little energy was dissipated at this stage. Deterioration of strength and stiffness was not very obvious. At the level of yielding, the hysteresis loops showed a much wider and thicker anti-S shape where the larger enclosed area of the loop indicated that much higher energy was dissipated compared with that of previous stages. These four specimens were shown to possess desirable seismic behavior.

The hysteresis loop of FB-2 had a relatively rapid drop of strength after reaching the maximum strength because of the small aspect ratio of 0.71. This indicated a relatively low capability of energy dissipation and ductility compared with that of FB-1. In spite of this, the wall could still

Table 2 Key factors on the behavior of specimens

| Direction	Specimens	Crack point		Yield point		Peak point		Ultimate point		μ
		F, kN	d, mm	F, kN	d, mm	F, kN	d, mm	F, kN	d, mm	
Positive (+)	FB-1	71.3	2.09	204.6	7.26	288.3	20.29	226.3	30.19	4.16
	FB-2	251.1	0.99	663.4	6.19	923.8	15.15	495	21.49	3.47
	FS-1	76	2.01	185.5	7.24	232.5	21.35	176.7	30.3	4.19
	FS-2'	306.9	0.89	—	—	—	—	—	—	—
	FS-2''	—	—	920.7	9.68	1207.9	24.73	1026.7	31.67	3.27
Negative (-)	FB-1	-60	-1.42	-220.1	-5.84	-279	-15.57	-238.7	-19.24	3.29
	FB-2	-248	-0.39	-663.4	-4.45	-858.7	-9.71	-561.1	-15.78	3.55
	FS-1	-68.2	-1.71	-130.2	-7.23	-210.8	-23.77	-173.6	-29.08	4.02
	FS-2'	-260.4	-0.57	—	—	—	—	—	—	—
	FS-2''	—	—	-936.2	-6.17	-1202	-18.28	-1143.9	-19.99	3.24
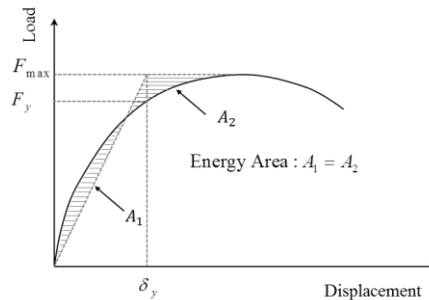
Fig. 12 Yield point determination

sustain cyclic load after the rapid drop of strength, and the enclosed area of the loop was still large, which indicated good ductility. The loop of FS-2 was unsymmetrical after the axial load was decreased because of the plastic deformation of the wall in the first loading. Displacements in the positive direction were greater than those in the negative direction.

8. Load-displacement responses

Measured displacement and lateral loads for the cracking, yielding, peak, ultimate points, and ductility capacity of the specimens are listed in Table 2. Yielding point was determined based on the equal energy area method, as shown in Fig. 12. Ultimate point was defined as the point on the envelope of the hysteretic curves at which the lateral load dropped to 80% of its maximum value (Park 1989). Displacement ductility was defined as the ratio of ultimate displacement to yield displacement. Load-displacement relationships of each specimen, which were obtained from the envelopes of the hysteretic curves, are shown in Fig. 13. The load-displacement curve of FS-2' and FS-2'' are both plotted.

It shows that the load-displacement envelops for one-bay structures were more stable than two-bay structures. The bearing capacities of the two-bay structures were about three to five times as much as those of one-bay structures, which indicated that aspect ratio had a significant effect on
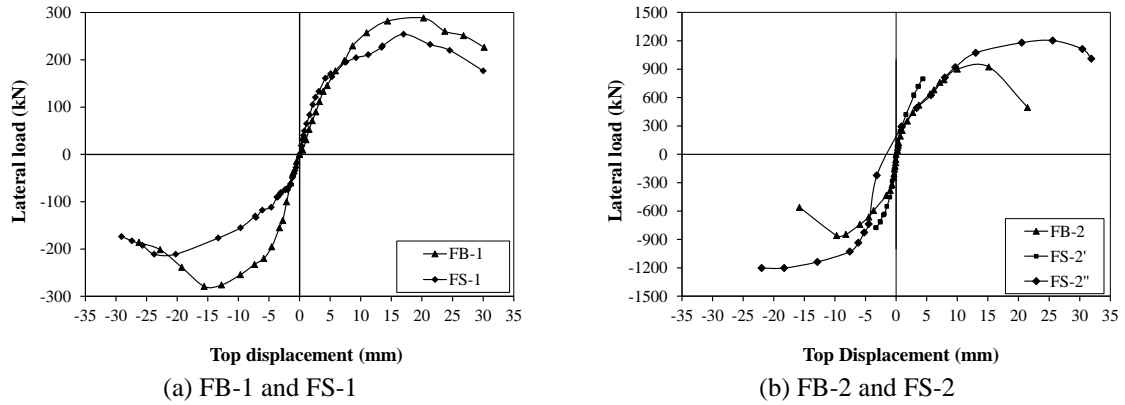
(a) FB-1 and FS-1   (b) FB-2 and FS-2

Fig. 13 Shear force-displacement envelope curves of specimens

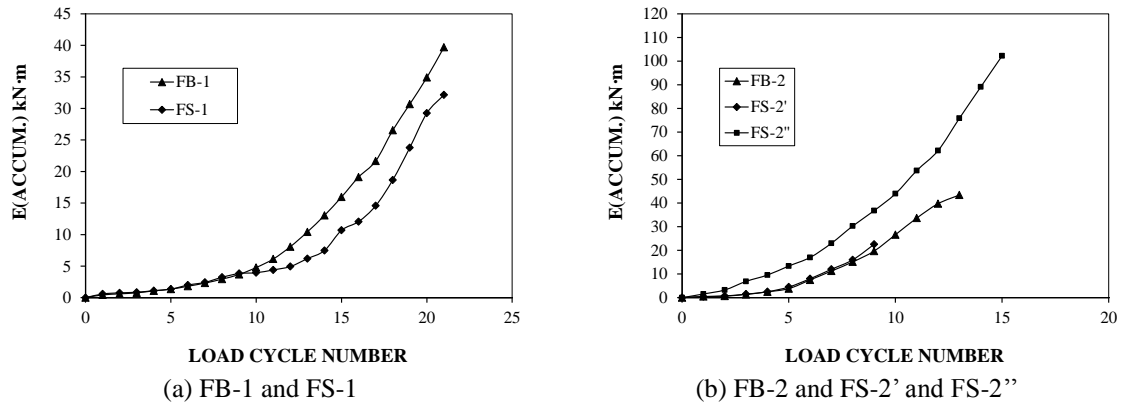(a) FB-1 and FS-1   (b) FB-2 and FS-2' and FS-2''

Fig. 14 Cumulative energy dissipated versus load cycle number

ductility and bearing capacity of the specimen. With the increase of aspect ratio, the bearing capacity improved as the ductility decreased. Moreover, the bearing capacity of specimen FB-1 was about 1.24 times as much as that of FS-1, whereas the bearing capacity of FS-2'' was about 1.3 times than that of FB-2. Ductility capacity of specimens FS-1 and FS-2 were basically the same as those of specimens FB-1 and FB-2, respectively. This showed that, the number of bays (one or two bay) affects the ductility capacity of the system. Also, the type of embedded wall affects the bearing capacity of the system more significantly.

9. Energy dissipation characteristics

Of particular significance to the seismic performance of RC walls is the energy dissipation capacity. There are different ways to evaluate the energy dissipation capacity of a structure. Energy dissipation of the test specimens under cyclic load in this study was defined as the area enclosed by the load-displacement hysteresis loops. Fig. 14 plots the cumulative dissipated energy versus the load cycle number for specimens FB-1, FS-1, FB-2, FS-2' and FS-2''. Because FS-2 was

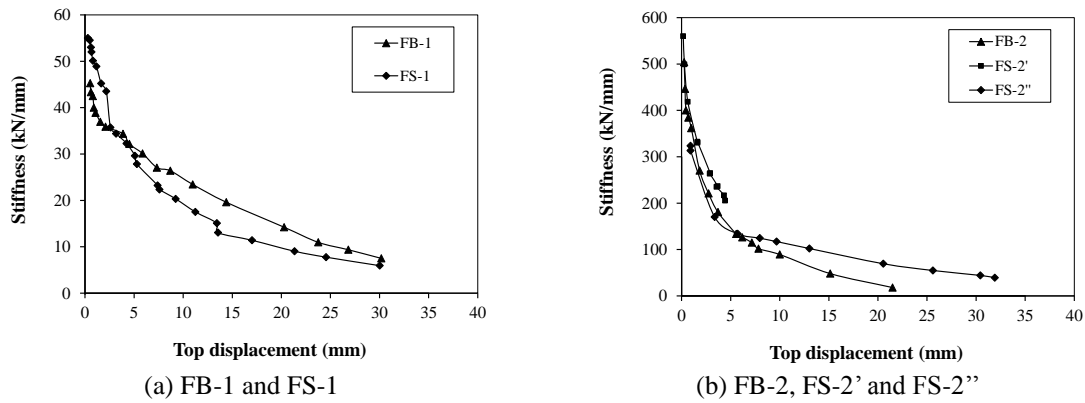(a) FB-1 and FS-1   (b) FB-2, FS-2' and FS-2''

Fig. 15 Secant stiffness versus top displacement

loaded twice, there are two energy dissipation curves for FS-2. In the parallel redundancy walls, two parts were nested to each other, and each part was independent and can withstand vertical and lateral loads alone. Therefore, an effective energy absorption mechanism was formed in which the weaker part would yield and fail first, thus absorbing a greater degree of the energy exerted by earthquakes. In FB-1, the barbell-shaped walls failed first, whereas in FS-1, the wall frame failed first. The dissipated cumulative energy corresponding to each load cyclic number was slightly larger in specimen FB-1 than in FS-1. This is because the barbell-shaped walls in FB-1 were more seriously damaged than the wall frame in FS-1, which dissipated more energy than FS-1. This indicates that embedded wall has a significant effect on the energy absorption mechanism of parallel redundancy walls. The energy capacity for FB-2 was quite similar with FS-2' when FS-2' had the same axial load with FB-2. This was because both of the walls were under very small displacement and the energy capacities for both walls were very low, the difference could not be seen clearly. However, when the axial load for FS-2'' was lowered down to 100 kN, the energy capacity for FS-2'' was much larger than FB-2. This indicates that axial load also has an influence on the energy dissipation capacity.

10 stiffness

Fig. 15 illustrates the variation of secant stiffness with top displacement of the four specimens. For reasons previously discussed, specimen FS-2 was loaded twice. The two cases of loadings of FS-2 are shown separately in Fig. 15 as FS-2' and FS-2''. For all the specimens, the stiffness gradually decreased. When the axial load ratio and aspect ratio were the same, the initial stiffness of wall frames with braced walls were larger than walls with barbelled walls. This is shown in Fig. 15, where the initial stiffness of FS-1 and FS-2' were 55 kN/mm and 560 kN/mm, which are larger than FB-1 (45 kN/mm) and FB-2 (504 kN/mm), respectively. However, FS-1 experienced greater stiffness deterioration than FB-1. This indicates that as the embedded walls get stronger, the initial stiffness becomes larger and stiffness deterioration becomes more serious. In addition, decreasing the axial load decreased the initial stiffness. This is also shown in Fig. 15. When axial load was decreased to 100 kN for FS-2, the initial stiffness was much smaller than FS-2' which held the axial load of 600 kN.

11. Conclusions

The results of an experimental research concerning the response of RC parallel redundancy walls subjected to in-plane cyclic loading have been presented herein. Parallel redundancy walls consist of two main parts nested to each other. These two parts have different mechanical behaviors and energy dissipation mechanisms. Each part is able to withstand vertical and lateral loads alone, and can play its own mechanical behavior. Based on the test results of specimens representing this concept, the following conclusions were made:

• The walls behaved as a "dual" lateral-load resisting system. In this dual system, both the wall frame and the embedded walls are involved in resisting lateral forces and there is a hierarchy in the failure process. The failure of one part led to the overall damage, whereas the other wall could still bear additional loads. In specimens FB-1 and FB-2, the wall frame still had a bearing capacity when the barbell-shaped walls were destroyed. On the contrary, in FS-1 and FS-2, the braced walls could still sustain loads after the failure of the wall frame. The combination of the two walls had a significant influence on the failure process.

• During the tests, the side wall columns developed horizontal cracks, and the embedded walls and the middle wall columns developed diagonal shear cracks in all four specimens, indicating the two parts of the parallel redundancy walls had different dissipation mechanisms.

• Hysteresis loops of four specimens showed wider and thicker shapes, indicating that the four specimens possessed desirable seismic behavior. The main parameters of the test were aspect ratio and embedded walls. Results showed that aspect ratio and embedded wall both have a significant effect on seismic behavior of the parallel redundancy walls. As the aspect ratio increases from 0.71 to 1.3, the specimens tended to have more stable hysteric behavior, greater ductility, and less stiffness deterioration. Seismic performance of parallel redundancy walls with high aspect ratio is better than those of low aspect ratio. In addition, as the embedded walls get stronger, the dissipation capacity becomes less.

• The tests indicated that the parallel redundancy wall is an efficient lateral load resisting component acting as a "dual" system with good ductility and energy dissipation capacity. Modifications in the embedded walls may be effectively made to improve seismic performance and to enhance ductility and energy dissipation capacity.

Acknowledgments

References

ASCE (2005), "Minimum design loads for buildings and other structures", ASCE/SEI 7-05, Reston, VA.

Berman, J.W. and Bruneau, M. (2005), "Experimental investigation of light-gauge steel plate shear walls", *J. Struct. Eng.*, **131**(2), 259-267.

Cao, W., Zhang, J., Dong, H. and Zheng, T. (2009), "Seismic performance of high rise shear wall with concealed truss", *J. Harbin Inst. Tech.*, **41**(4), 153-158. (in Chinese)

Cennamo, C., Cennamo, G.M. and Chiaia, B.M. (2012), "Robustness-oriented design of a panel-based

shelter system in critical sites", *J. Arch. Eng.*, **18**(2), 123-139.

Clayton, P.M., Winkley, T.B., Berman, J.W. and Lowes, L.N. (2012), "Experimental investigation of self-centering steel plate shear walls", *Structures Congress 2012 - Proceedings of the 2012 Structures Congress*, Chicago, March.

Dong, H. (2002), "Design theory and experiment study on seismic behavior of RC coupled shear wall with concealed bracings", Ph.D. Dissertation, Beijing University of Technology, Beijing. (in Chinese)

FEMA (1997), "NEHRP guild lines for the seismic rehabilitations of buildings", NEHRP 1997 (FEMA-273), Washington, D.C.

FEMA (2003), "NEHRP recommended provisions for seismic regulations for new buildings and other structures", NEHRP 2003 (FEMA-450), Washington, D.C.

GB 50010 (2010), "Code for design of concrete structures", China Architecture & Building Press, Beijing. (in Chinese)

GB 50011 (2010) "Code for seismic design of buildings", China Architecture & Building Press, Beijing. (in Chinese)

International Conference of Building Officials (ICBO) (1997), "Uniform building code (UBC-97)", Whittier, California.

Jiang, H., Lu, X.L, Kwanand, A.K.H. and Cheung, Y.K. (2003), "Study on a seismic slit shear wall with cyclic experiment and macro-model analysis", *Struct. Eng. Mech.*, **16**(4), 371-390.

Kaltakci, M.Y. and Yavuz, G. (2012), "An experimental study on strengthening of vulnerable RC frames with RC wing walls", *Struct. Eng. Mech.*, **41**(6), 691-710.

Kanno, Y. and Ben-Haim, Y. (2011), "Redundancy and robustness, or when is redundancy redundant", *J. Struct. Eng.*, **137**(9), 935-945.

Kwan, A.K.H., Lu, X.L. and Cheung, Y.K. (1993), "Elastic analysis of slitted shear walls", *Int. J. Struct.*, **13**(2), 75-92.

Liao, K., Wen, Y. and Foutch, D.A. (2007), "Evaluation of 3D steel moment frames under earthquake excitations. II: reliability and redundancy", *J. Struct. Eng.*, **133**(3), 471-480.

Lu, X. and Wu, X. (2000), "Study on a new shear wall system with shaking table test and finite element analysis", *Earthq. Eng. Struct. Dyn.*, **29**(10),1425-1440.

Park, R. (1989), "Evaluation of ductility of structures and structural assemblages from laboratory testing", *Bul. NZ Nat. Soc. Earthq. Eng.*, **22**(3), 155-166.

Qu, B., Bruneau, M., Lin, C. and Tsai, K. (2008), "Testing of full-scale two-story steel plate shear wall with reduced beam section connections and composite floors", *J. Struct. Eng.*, **134**(3), 364-373.

Riva, P. and Franchi, A. (2001), "Behavior of reinforced concrete walls with welded wire mesh subjected to cyclic loading", *ACI Struct. J.*, **98**(3), 324-334.

Sittipunt, C., Wood, S.L., Lukkunaprasit, P. and Pattararattanakul, P. (2001), "Cyclic behavior of reinforced concrete structural walls with diagonal web reinforcement", *ACI Struct. J.*, **98**(4), 554-562.

Sun, G., He, R., Gu, Q. and Fang, Y. (2011), "Cyclic behavior of partially-restrained steel frame with RC infill walls", *J. Construct. Steel Res.*, **67**(4), 1821-1834.

Tong, X., Hajjar, J.F., Schultz, A.E. and Shield, C.K. (2005), "Cyclic behavior of steel frame structures with composite reinforced concrete infill walls and partially-restrained connections", *J. Construct. Steel Res.*, **61**(1), 531-52.

Wen, Y.K. and Song, S.H. (2003), "Structural reliability/redundancy under earthquakes", *J. Struct. Eng.*, **129**(1), 56-67.

Ye, L. and Kang, S. (2001), "Seismic behavior of dual function slitted shear wall", *J. Tsinghua Sci. Tech.*, **6**(5), 453-457.

Zhao, Q. and Astaneh-Asl, A. (2004), "Cyclic behavior of traditional and innovative composite shear walls", *J. Struct. Eng.*, **130**(2), 271-284.

CC